Fluorescence Anisotropy Decay of Ethidium Bound to Nucleosome Core Particles. 1. Rotational Diffusion Indicates an Extended Structure at Low Ionic Strength†

David W. Brown, Louis J. Libertini, and Enoch W. Small*
Department of Biochemistry and Biophysics, Oregon State University, Corvallis, Oregon 97331-6503
Received December 7, 1990; Revised Manuscript Received March 4, 1991

ABSTRACT: The fluorescence decay of ethidium intercalated into the DNA of nucleosome core particles increases in average lifetime from about 22 ns in H_2O to about 39 ns in D_2O. This increase, combined with the acquisition of large amounts of data (on the order of 10^8 counts per decay), allows measurement of anisotropy decays out to more than 350 ns. The overall slow rotational motions of the core particle may thereby be more clearly distinguished from the faster torsional motions of the DNA. In 10 mM NaCl at 20 °C, we recover a long correlation time of 198 ns in D_2O (159 ns when corrected to a viscosity of 1.002 cP), in agreement with the value of 164 ns obtained in H_2O. These values are consistent with hydrodynamic calculations based on the expected size and shape of the hydrated particle. To support our conclusion that this long correlation time derives from Brownian rotational diffusion, we show that the value is directly proportional to the viscosity and inversely proportional to the temperature. No significant changes in the rotational correlation time are observed between 1 and 500 mM ionic strength. Below 1 mM, the particle undergoes the "low-salt transition" as measured by steady-state tyrosine fluorescence anisotropy. However, we observe little change in shape until the ionic strength is decreased below ~0.2 mM, where the correlation time increases nearly 2-fold, indicating that the particle has opened up into an extended form. We have previously shown that the transition becomes nonreversible below 0.2 mM salt.

Nucleosome core particles are subunits of chromatin structure consisting of a 146 base pair (bp)[1] segment of DNA wrapped around a protein core composed of two each of the histones H2A, H2B, H3, and H4. The results of early hydrodynamic studies, together with later neutron diffraction, electron microscopy, and X-ray diffraction studies, have all combined to provide a general picture of the structure of the core particle complex. The model which has arisen shows the core particle to be roughly disk-shaped, with a diameter of 110 Å and a thickness of 57 Å [for a review, see van Holde (1988)].

A large fraction of the eukaryotic genome, including both active and inactive genes, is organized into nucleosomes; the biological functions of chromatin (i.e., replication, transcription, repair, etc.) will require mechanisms for the transient unraveling of this structure. The nucleosome core particle has been shown to undergo several different in vitro conformational transitions in response to changes in the solvent environment. Although the conditions required to induce many of the observed transitions are far from physiological, the nature of the changes involved are of interest because they reflect alterations in histone–histone or histone–DNA interactions which might also be possible in vivo. For this reason, a number of laboratories, including our own, have been examining such transitions by a variety of methods.

The low-salt transition of nucleosome core particles has been extensively studied, and several conflicting reports have appeared in the literature. Our laboratory has performed a number of studies in order to characterize this transition and to try to resolve some of these conflicts (Libertini & Small, 1980, 1982, 1984a, 1987a; Small et al., 1988, 1991; Brown et al., 1990). One facet of the transition which has received considerable attention is the change in shape of the particle. That this transition involves a substantial unfolding of the core particle was demonstrated by Wu et al. (1979) and by Burch and Martinson (1980), who found that it was completely inhibited by dimethyl suberimidate cross-linking of the core histones. Early electric dichroism studies indicated a large change in the dipole moment and rotational diffusion coefficient, consistent with a major opening of the core particle (Wu et al., 1979). On the other hand, later studies using low-angle neutron scattering by Mita et al. (1983), Uberbacher et al. (1983), and Hirai et al. (1988) report only small changes in the radius of gyration of the particle at low ionic strength and conclude that there is very little shape change occurring.

High-salt unfolding and dissociation have been studied by sedimentation, CD spectroscopy, and ^1H NMR; the data all point to a loosening of the core particle structure at ionic strengths >500 mM as a result of weakened protein–DNA interactions [reviewed in van Holde (1988)]. At salt concentrations >800 mM, a stepwise removal of the core histones is observed as the particle begins to dissociate (Burton et al., 1978).

Decay of fluorescence anisotropy provides a means of measuring rotational diffusion of macromolecules. The rotational diffusion coefficients obtained are very sensitive to shape and size (Small et al., 1991); small changes in the macromolecule can result in significant changes in the anisotropy decay. Most of our earlier work involved measurements of the intrinsic tyrosine fluorescence. However, tyrosine fluorescence decays with too short a lifetime (only 1–2 ns) to be useful for measurements on the time scales necessary for the determination of core particle rotational diffusion; we have instead utilized the intercalating dye ethidium bromide as a probe of these rotational motions.

Ethidium is a fluorescent molecule which binds to DNA in solution by intercalation between adjacent base pairs. Such

† This work was supported by NIH Grant GM25663. D.W.B. also received support from NIH Predoctoral Training Grant GM07774.

[1] Abbreviations: bp, base pair(s); H2A, H2B, H3, and H4, histones H2A, H2B, H3, and H4, respectively; SDS, sodium dodecyl sulfate; PAGE, polyacrylamide gel electrophoresis; ϕ_{max}, maximum anisotropy decay lifetime obtained from method of moments or least-squares analysis; [M^+], cation concentration.

0006-2960/91/0430-5293$02.50/0

binding results in a large increase in the fluorescence quantum yield with the decay lifetime increasing to about 22 ns from a value of about 1.6 ns (unpublished observation) for free ethidium. Ethidium also binds readily to the core particle, with changes in fluorescence properties similar to those which occur upon binding to free DNA (Ashikawa et al., 1983; Genest et al., 1982). These changes suggest that binding to the core particle also occurs by intercalation into the DNA. Recent studies involving tritiated azidoethidium covalently bound to core particles support the conclusion that ethidium binds to the DNA with little or no binding to the protein (McMurray et al., personal communication).

The fluorescence anisotropy of ethidium bound to core particles will decay in response to all of the various depolarizing motions that the moiety can undergo during the lifetime of the excited state. These motions can be classified as (1) subnanosecond wobbling motions of the ethidium within its binding site (Millar et al., 1980; Magde et al., 1983), (2) slower torsional motions of the DNA on an intermediate time scale (Genest et al., 1982; Wang et al., 1982; Ashikawa et al., 1983; Schurr & Schurr, 1985; Wahl et al., 1970; Winzeler & Small, 1991), and (3) very slow motions due to overall rotational diffusion of the particle on a time scale of hundreds of nanoseconds. Early studies using the fluorescence anisotropy decay of ethidium bound to nucleosomes (Ashikawa et al., 1983; Genest et al., 1982) concentrated on the DNA flexing motions, because these occur in time scales accessible to their measurements.

In some of the experiments presented here, we have extended the time range accessible in the anisotropy decay by substituting D_2O for H_2O. In D_2O, the lifetime of DNA-bound ethidium increases to nearly 40 ns, due to a reduced exchange rate of deuterons between the solvent and the excited-state chromophore (Olmsted & Kearns, 1977). Combined with the use of a high repetition rate picosecond laser as the excitation source and long data collection times, the use of D_2O as a solvent extends the time range available for ethidium fluorescence decay measurements to more than 350 ns. This extended time scale diminishes the degree to which torsional flexing of the DNA will interfere with observation of the effects of rotational diffusion. Since experiments in both D_2O and H_2O recover the same rotational diffusion properties, we conclude that, even when H_2O is used as the solvent, the rotational motions of the core particle may be studied by using ethidium fluorescence.

In this work, we first show that ethidium fluorescence may be used to obtain accurate information on the rotational motions of nucleosome core particles. We then examine the effects of a wide range of salt concentrations on these rotational motions, with a particular emphasis on low ionic strengths.

Materials and Methods

Materials

Deuterium oxide (D_2O), erythrosin B, and calf thymus DNA were from Sigma Chemical; ethidium bromide was from Molecular Probes.

Chicken erythrocyte core particles were prepared as previously described (Libertini & Small, 1980; Libertini et al., 1988). This procedure involves a brief predigestion of extracted chromatin with micrococcal nuclease, extraction of the noncore chromosomal proteins with CM-Sephadex, final nuclease digestion to monomer core particles, and purification by gel-exclusion chromatography on Sepharose 6B-CL. Visualization of the proteins by using SDS–PAGE showed only the four core histones present in equal amounts; native PAGE of DNA extracted from the core particles after Pronase digestion of the histones or by hydroxylapatite chromatography (Hirose, 1988) resolved as a single band with a size of 146 ± 2 bp (results not shown). Concentrated stock solutions of the core particles were prepared by using an Amicon Centricon microconcentrator.

Methods

Data Collection. Steady-state tyrosine fluorescence intensity and anisotropy were measured as described previously (Libertini & Small, 1982; Libertini et al., 1988).

Fluorescence decay measurements were made on a lifetime fluorometer using a synchronously pumped, cavity-dumped picosecond dye laser as the light source. This instrument and recent modifications have been described (Small & Anderson, 1988; Small, 1991a). In order to adequately excite ethidium fluorescence, it was necessary to operate the dye laser with rhodamine 575 in place of the more usual rhodamine 6G in order to extend its response to the blue (Libertini & Small, 1987b). Samples were excited with vertically polarized light at 556 nm. The fluorescence was isolated by using a Corning CS 2-73 cutoff filter (50% transmittance at 585 nm) in combination with a 593-nm band-pass filter (transmission half-width ~15 nm) and detected with a Hamamatsu R1645U-07 red-sensitive, dual microchannel plate photomultiplier tube. The dye laser pulse rate was 800 kHz, and the excitation intensity was adjusted to give a data collection rate of about 20 kHz. These settings would result in a multiphoton event rate on the order of 1.2% of total counts; through the use of energy windowing, we are able to decrease the proportion of multiphoton events to an estimated 0.4% contamination (Hutchings & Small, 1990).

Data sets consist of 3 separate decays, each containing 1024 channels of data collected at a channel width of 0.376 ns/channel. The first decay, $E(t)$, was usually obtained by using the decay of erythrosin in water. Due to its extremely short lifetime [$\tau \approx 0.09$ ns (Libertini & Small, 1984b)], this decay is nearly indistinguishable from the instrument response typically measured; in addition, the erythrosin decay can be collected through the identical filter setup used for the collection of the ethidium decays, thus eliminating one possible source of error. The second and third decays are $F_{\parallel}(t)$ (the fluorescence emission of the sample collected through a vertically oriented polarizer) and $F_{\perp}(t)$ (fluorescence emission through a horizontally oriented polarizer). To reduce errors due to possible instrumental "drift" or laser fluctuation during the extended periods of measurement, $E(t)$, $F_{\parallel}(t)$, and $F_{\perp}(t)$ were collected alternately for 10–15 min periods and the results summed to form the complete data set.

A primary background for each sample was estimated by blocking the excitation beam outside of the instrument and collecting data. The average number of counts per channel obtained, corrected to the total time of collection, was then subtracted from each decay. Counting rates from samples of core particles in the absence of ethidium were low and consisted mainly of scattered light; thus, no correction for background from this source was necessary.

Data Corrections. The pulse rate of the mode-locked Nd:YAG pump laser is 81.5 MHz, which is also the repetition rate of the dye laser. The cavity dumper on the dye laser reduces this pulse rate (to 800 kHz in our case) through the use of an acousto-optical device called a Bragg cell. Ideally, the Bragg cell deflects only the desired pulses out of the dye laser cavity (Small, 1991a). However, secondary pulses, nearly 5 orders of magnitude lower in intensity than the main pulse and spaced at an interval of ~12.3 ns (corresponding to the

pulse period of the pump laser), also leak through and can be observed in the measured $E(t)$.

These secondary pulses contribute significantly to the fluorescence decay of the sample at long times and will thus distort the anisotropy decay calculated as described below. In order to minimize this distortion, we generate correction files which represent estimated contributions to the fluorescence of all of the secondary pulses. Correction then involves subtracting the corresponding correction files from the original $E(t)$, $F_{\parallel}(t)$, and $F_{\perp}(t)$ data files. To generate the correction files, we first determine the number of counts (N_i) in each secondary peak of $E(t)$ relative to the number in the main peak (N_o). Then, for each secondary peak, $E(t)$, $F_{\parallel}(t)$, and $F_{\perp}(t)$ are multiplied by the peak ratio (N_i/N_o) and summed into respective correction files after being shifted so as to match the main peak position to the secondary peak in the unmodified $E(t)$. The adequacy of this *numerical correction for the convolution artifact* was demonstrated by using simulated, noiseless data comparable to the experimental results which we show below.

Even after correction for background and for the secondary excitation peaks, visual examination of the decays at long times showed that they did not decay completely to zero as expected. An additional correction was therefore made for this small (10–30 counts per channel for decays containing 75 million total counts) residual background level. Correction was made by estimating the "secondary background" using a simple two-component least-squares analysis on the tails of the decays with one lifetime fixed at 10^6 ns; the resulting preexponential factors corresponding to the fixed lifetime were then subtracted from the decays before proceeding. Efforts to determine the source of this extremely low-level "secondary background" have been unsuccessful.

An overall sensitivity correction, S, is also needed. This factor corrects for (1) the differential instrumental sensitivity between the two polarization components, (2) the practice of collecting $F_{\parallel}(t)$ and $F_{\perp}(t)$ at approximately equal counting rates, and (3) any difference in the number of counts collected in $F_{\parallel}(t)$ and $F_{\perp}(t)$. The method used is described in Small and Anderson (1988).

Calculations. After corrections for primary background, secondary pulsing, and secondary background [yielding $F'_{\parallel}(t)$ and $F'_{\perp}(t)$], the total fluorescence intensity decay (which will have no contribution from the decay of the anisotropy) is calculated as

$$F'_t(t) = F'_{\parallel}(t) + 2SF'_{\perp}(t) \quad (1)$$

The anisotropy decay can then be approximated by

$$r'(t) = \frac{F'_{\parallel}(t) - SF'_{\perp}(t)}{F'_t(t)} \quad (2)$$

This approximation should be quite good since we are using a fast laser source and a microchannel plate detector (Small, 1991a). Use of eq 1 and 2 effectively separates the contributions of the intensity decay and the anisotropy decay, permitting them to be analyzed separately. The resulting analyses are thus greatly simplified as compared to direct deconvolution of $F_{\parallel}(t)$ and $F_{\perp}(t)$, which, for the type of data presented here, would require simultaneously solving for at least 12 parameters [three exponential decay times and 3 preexponential factors for each of $F_t(t)$ and $r(t)$]. Analyses of simulated fluorescence decay data [$F_{\parallel}(t)$ and $F_{\perp}(t)$] demonstrated that use of eq 2 to approximate the anisotropy decay does not introduce significant distortions for our purposes since decay components with lifetimes lower than 2 ns could be accurately recovered. It is important to note, however, that the usefulness of eq 2 for experimental data depends critically on the correction described above for secondary pulses in the excitation and to a lesser degree on the secondary background correction.

Data Analysis. Total fluorescence decays, $F'_t(t)$, were analyzed as sums of exponentials using method of moments deconvolution with λ invariance (Small, 1991b; Small et al., 1989; Isenberg & Small, 1982). Distribution analyses of the total decays were performed by using the method of moments as recently described (Libertini & Small, 1989). Anisotropy decays were analyzed directly (no deconvolution) by both a method of moments and a least-squares fitting method. The least-squares analysis program was based on the Marquart search algorithm as described by Bevington (1969). In all cases, the method of moments and least-squares analyses gave comparable results for ϕ_{max}, the longest recovered anisotropy decay lifetime.

The deviation, d_i, of the calculated fits to the anisotropy decay data was computed as

$$d_i = \frac{r_i - s_i}{v_i^{1/2}} \quad (3)$$

where r_i, s_i, and v_i are the experimental result (the anisotropy decay data calculated from eq 2), the calculated fit (sum of exponentials from the method of moments or least-squares analysis), and the variance of the experimental result at channel i, respectively. The variance (v_i) was calculated by using standard error progression and the assumption that the variance of F'_i is equal to F'_i + background for the corrected decay data ($\parallel$ and $\perp$ components). Omitting the "i" subscript from v, F'_t, $F'_{\parallel}$, and $F'_{\perp}$ for simplicity:

$$v = \frac{9S^2[(F'_{\parallel} + b)F'^2_{\perp} + (F'_{\perp} + c)F'^2_{\parallel}]}{F'^4_t} \quad (4)$$

where b and c are the total backgrounds (primary + secondary) subtracted to give $F'_{\parallel}$ and $F'_{\perp}$, respectively. Calculation of the fitting parameter (reduced χ^2 value) used in the least-squares analysis program included v_i as the weighting factor for the squared residuals.

Results

Fluorescence Intensity Decay of Ethidium Bound to Core Particles. The high repetition rate of our cavity-dumped dye laser (800 kHz) allows us to collect on the order of 100 million monophoton fluorescence events each in $F_{\parallel}(t)$ and $F_{\perp}(t)$ during a 3–4-h period. After data correction as described above, these two decays can be combined by using eq 1 to yield $F'_t(t)$, the total fluorescence decay. Examples of $F'_t(t)$ are plotted on a log scale in Figure 1 for ethidium bound to core particles in H_2O and D_2O. Two features of these decays are noteworthy. First, the total fluorescence is detectable over more than 4 orders of magnitude before decaying off into background noise. Second, even with this large amount of data, the decays appear to be approximately straight lines, showing that the they are, to a first approximation, nearly monoexponential.

Initial analyses of these decays as sums of exponentials indicated at least three components—a well-resolved long lifetime, a less well resolved intermediate lifetime, and a poorly resolved short lifetime making only a small contribution. To improve the resolution of the intermediate decay lifetime, we tried fixing the short lifetime using the filter method of Cheng and Eisenfeld (1970) which does not restrict the corresponding preexponential factor (α). We have previously shown this method to be very effective for the resolution of closely spaced decays (Libertini & Small, 1983). The effect of the fixed

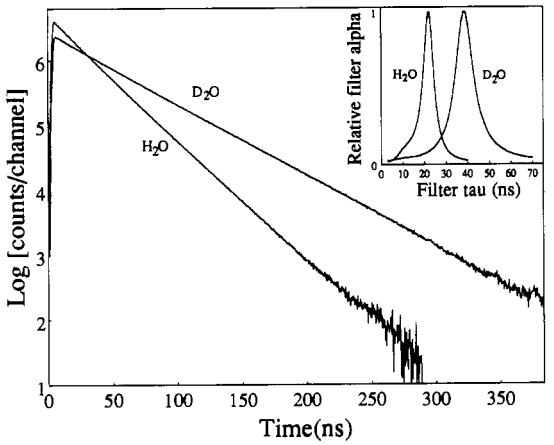

FIGURE 1: Total fluorescence decays, $F'_{\parallel}(t)$, of ethidium bound to chromatin core particles in H_2O and D_2O. Samples were prepared by adding core particles to a buffer solution to give final concentrations of 0.6 μM core particles, 0.2 mM Tris–cacodylate, 0.73 μM ethidium bromide, and 10 mM NaCl in either H_2O or D_2O; the pH and pD values were estimated to be 6.5 and 6.9 (Covington et al., 1968), respectively. All samples were equilibrated 60–80 min at room temperature prior to measurement; the temperature during measurement was kept constant at 20 °C. The summed data sets contained approximately 2.5×10^8 total counts. The inset shows results obtained from distribution analyses of the summed decays (Libertini & Small, 1989).

Table I: Analysis Results on Total Fluorescence Intensity Decays of Ethidium Bound to Core Particles or Free DNA

sample		component[a] 1	2	3	τ_{av}[b]
core particles in H_2O[c]	α_i	trace	0.35	1.00	
	τ_i	<5	15.4	23.9	22.3
core particle DNA in H_2O[d]	α_i	trace	0.30	1.00	
	τ_i	<5	17.0	24.4	23.1
core particles in D_2O[e]	α_i	trace	0.13	1.00	
	τ_i	<3	25.9	40.4	39.3
core particle DNA in D_2O[f]	α_i	trace	0.08	1.00	
	τ_i	<7	25.5	41.1	40.3
calf thymus DNA in D_2O[g]	α_i	trace	0.09	1.00	
	τ_i	<7	24.8	41.4	40.6

[a] Parameters listed were obtained by using Cheng–Eisenfeld filters for the lifetime of the trace component in order to improve the resolution of the major components (see text). Results were essentially independent of the value chosen for the filter within the range shown. [b] Intensity-weighted average liftime $[\tau_{av} = (\alpha_2\tau_2^2 + \alpha_3\tau_3^2)/(\alpha_2\tau_2 + \alpha_3\tau_3)]$ for the major components. [c] A total of 243 million counts, 3.9 million in the peak channel. Decay shown in Figure 1. [d] Prepared by hydroxylapatite chromatography; [NaCl] = 100 mM. A total of 125 million counts, 1.9 million in the peak channel. [e] A total of 245 million counts, 2.3 million in the peak channel. Decay shown in Figure 1. [f] Prepared by Pronase digestion followed by standard phenol/chloroform extraction; [NaCl] = 10 mM. A total of 260 million counts, 2.4 million in the peak channel. [g] [NaCl] = 10 mM. A total of 250 million counts, 2.2 million in the peak channel.

lifetime was examined over a range of values in an effort to find the one giving the most stable result according to the rules of method of moments. The results are listed in Table I. Only a maximum value is listed for the trace decay lifetime since the α and τ values obtained for the two major components were relatively independent of the set filter lifetime. Table I also includes results obtained with ethidium bound to free core particle DNA and to high molecular weight calf thymus DNA. Although the parameters obtained with free DNA are very similar to those obtained for the core particle decays, the free DNA samples exhibit somewhat higher lifetimes, clearly apparent in the averages listed. While small, this difference is consistently observed and may indicate that the binding sites of ethidium on core particles are somewhat more exposed to quenching than those on free DNA.

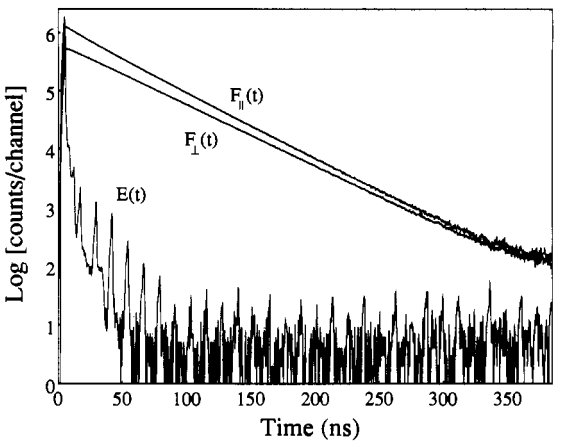

FIGURE 2: Raw fluorescence data for ethidium bound to chromatin core particles in D_2O. The sample was the same as that used for Figure 1. $E(t)$ is the measured excitation; $F_{\parallel}(t)$ and $F_{\perp}(t)$ are the decays obtained with the emission polarizer parallel or perpendicular to the excitation polarization direction.

There are a wide variety of possible binding sites for ethidium intercalated in random-sequence DNA. Due to possible differences in the degree of quenching, such variety could result in a large number of closely spaced lifetimes contributing to the intensity decay. The inset to Figure 1 shows the results of analyses of the intensity decays in terms of a continuous distribution of lifetimes (Libertini & Small, 1989). The results indicate narrow, nearly symmetrical distributions with only slight skewing to shorter lifetimes. As expected, the peaks of the distributions fall near the average of the lifetimes listed in Table I.

Anisotropy Decay Is Dominated by a Single Long Correlation Time. Figure 2 illustrates the raw fluorescence data $[E(t), F_{\parallel}(t)$, and $F_{\perp}(t)]$ obtained from a sample of ethidium bound to core particles in D_2O. The regularly spaced spikes (secondary pulses) following the main pulse in $E(t)$ are due to leakage of light from the cavity-dumped dye laser; the correction of their contribution to the fluorescence decays is discussed under Materials and Methods. It should again be noted that the data are presented on a log scale to demonstrate the monoexponential appearance of the decays. Significant in this figure is the fact that $F_{\parallel}(t)$ and $F_{\perp}(t)$ both show very little noise even 375 ns beyond the initial excitation, almost 10 times the lifetime of the DNA-bound probe in D_2O. Similar data from core particles in H_2O (not shown) decay off into background noise at around 250 ns (as in Figure 1).

The anisotropy decay is a function of the difference between the two fluorescence decay components (see eq 2) and is therefore intrinsically much noisier than the total fluorescence. For measurements of rotational diffusion, the intensity decay lifetime of the ideal probe would be comparable to the rotational correlation time for the macromolecule of interest. When it is much smaller, as is usually the case here, it becomes necessary to collect a very large number of counts in the intensity decay components in order to improve the signal-to-noise level and extend the useable range of the anisotropy decay to longer times.

Figure 3A shows anisotropy decays for ethidium bound to core particles in H_2O and D_2O at 20 °C. When plotted on a log scale, the shape is marked by an initial curvature out to ~50 ns, followed by a slower, apparently linear decrease out to the limits of the data. We analyzed these decays as simple sums of exponentials; the results obtained from method of moments analysis are shown in Table II and and are sup-

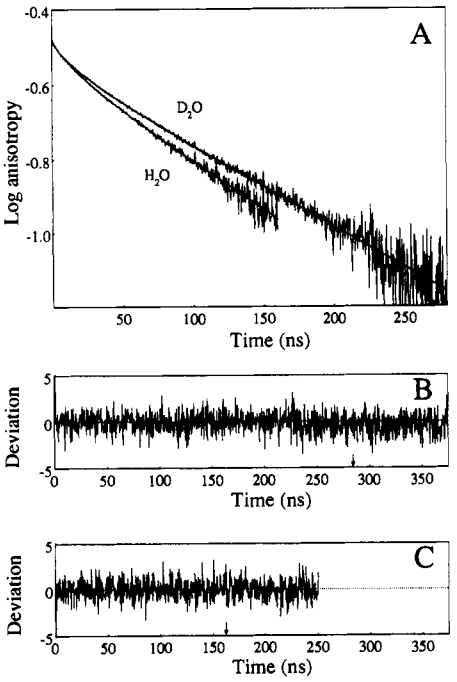

FIGURE 3: Examples of fluorescence anisotropy decays of ethidium bound to core particles. (A) shows anisotropy decays in H_2O and D_2O, along with calculated curves derived from analyses of the data. Samples contained 0.6 μM core particles, 0.18 μM ethidium bromide, and 10 mM NaCl. (A) Anisotropy decays; for clarity, only data for the channel range analyzed are displayed. (B) Deviation plot for the result in D_2O. (C) Deviation plot for the result in H_2O. Note that in (B) and (C) deviations are included for much wider channel ranges than used for analysis; the last channel used for analysis is marked by an arrow.

Table II: Results of Analyses on Anisotropy Decays for Ethidium Bound to Core Particles[a]

solvent		component 1	component 2	component 3 (ϕ_{max})
H_2O	β_i	0.016	0.037	0.29
	ϕ_i	3	18	164
D_2O	β_i	0.013	0.036	0.29
	ϕ_i	4	21	198.5

[a] The decays analyzed are those shown in Figure 3.

ported by results of least-squares analyses. The smooth curves included in Figure 3A are those calculated from the parameters in the table. Deviation plots, based on eq 3 and 4 and shown as Figure 3B,C, indicate an excellent correspondence with the experimental decays at long times.

The anisotropy decays are dominated by a single, long decay lifetime (ϕ_{max}) which we attribute to rotational tumbling of the core particle and is well resolved from the other components of the decay. Support for this assignment will be detailed under Discussion. The two minor components are presumed to represent anisotropy decay arising from the torsional twisting and bending motions of the DNA. Although the fit to the data is excellent, representation of such complex motions by a sum of two exponentials is clearly simplistic. We will make no attempt to discuss these motions in this report; the following paper in this series (Winzeler & Small, 1991) details more rigorous analyses of the torsional motions of the DNA according to a model described by Schurr (Schurr, 1984; Schurr & Schurr, 1985).

The effects of viscosity and temperature on ϕ_{max} are presented in Figure 4 as a plot of $1/\phi_{max}$ against T/η. A simple linear fit of the points is shown by the straight line. The observed linear dependence provides evidence that ϕ_{max} is

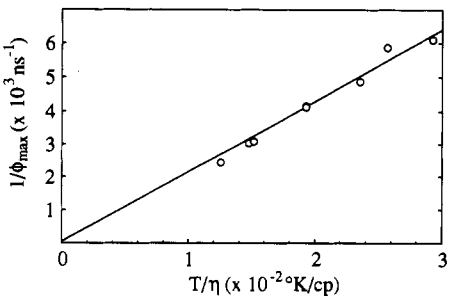

FIGURE 4: Reciprocal of the longest recovered anisotropy decay lifetime of chromatin core particles (ϕ_{max}) plotted as a function of T/η. From left to right, the samples were in (a) H_2O at 7.1 °C with 14.2% sucrose, η = 2.236 cP; (b) D_2O at 6.5 °C, η = 1.891 cP; (c) H_2O at 13.1 °C with 14.2% sucrose, η = 1.889 cP; (d) H_2O at 6.5 °C, η = 1.450 cP; (e) [coincident with (d)] H_2O at 20 °C with 13.7% sucrose, η = 1.519 cP; (f) D_2O at 20 °C, η = 1.247 cP; (g) D_2O at 23 °C, η = 1.152 cP; and (h) H_2O at 20 °C, η = 1.002 cP. Viscosities for samples in H_2O were estimated from the CRC Handbook of Chemistry and Physics, 60th edition; viscosities for D_2O were calculated by using equations presented by Matsunaga and Nagashima (1983). Samples contained 0.6 μM core particles, 10 mM NaCl, and ethidium bromide at 0.18 μM (samples a–e), 0.7 μM (f, h), or 0.07 μM (g).

indeed a measure of the rotational correlation time of the core particle.

Value of ϕ_{max} Is Insensitive to pH. Core particles have been found to undergo a transition with increasing pH, centered near pH 7 and characterized by small changes in the circular dichroism of the DNA and in the steady-state fluorescence anisotropy of the intrinsic tyrosine residues (Libertini & Small, 1984a). The results suggested that core particles have a somewhat looser structure at higher pH. Although the sedimentation coefficient did not show any significant effect of pH, rotational diffusion is considerably more sensitive to size and shape. We therefore examined the effect of pH on the anisotropy decay of ethidium bound to core particles at 10 mM ionic strength. No significant pH dependence was found for ϕ_{max} (results not shown). There were, however, significant effects observed for the two shorter recovered lifetimes. As stated above, we attribute these to the torsional motions of the DNA and do not characterize them here. As will be shown in the companion paper, significant effects of pH on the torsional motions of the DNA can be characterized (Winzeler & Small, 1991).

Core Particle at Very Low Ionic Strength. When the ionic strength is reduced below about 3 mM, we have observed core particles to undergo a transition characterized by changes in steady-state tyrosine fluorescence anisotropy and intensity, in circular dichroism of the DNA, and in sedimentation coefficient. The results suggest an opening of the core particle with decreasing salt concentration (Libertini & Small, 1982; Libertini et al., 1988). An example of the results obtained with tyrosine anisotropy in the presence of ethidium is shown in Figure 5A (filled circles). Results from a control experiment done in the absence of ethidium are also shown (plus symbols) and demonstrate that binding of ethidium at the ratio of 0.3 per core particle has no significant effect on the shape or extent of the "low-salt transition". Even at a binding ratio of 1.2 ethidiums per core particle, the transition is relatively unaffected—a ~30% decrease in the overall change of anisotropy is observed (not shown). Nevertheless, one must keep in mind the possibility that core particles with an ethidium bound may respond somewhat differently to low ionic strength than those without.

In the following experiments, it would have been preferable to use D_2O as the solvent in order to extend the time range of the anisotropy decay data obtained and thus better define

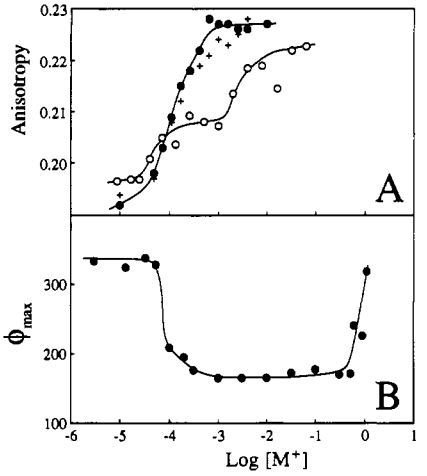

FIGURE 5: Effects of ionic strength on the steady-state tyrosine fluorescence anisotropy (A) and on ϕ_{max} (B) for nucleosome core particles. A concentrated stock of core particles in 1 mM Tris-HCl, pH 8.0, was prepared by repeated washings using a Centricon microconcentrator. Filled circles are results obtained when this stock was diluted directly into solutions of the given ionic strength. Open circles are results obtained for samples first diluted into distilled water to obtain the very low ionic strength; after 1 h at room temperature, NaCl at 10 times the final concentrations was added to give the indicated ionic strength. Samples contained 0.6 μM core particles, 0.18 μM ethidium bromide, 0.003 mM Tris-HCl, and NaCl to give the indicated final [M+].

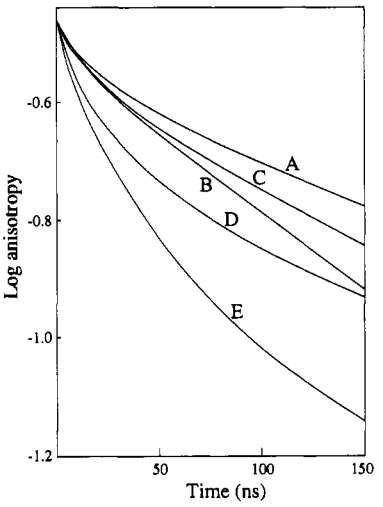

FIGURE 6: Anisotropy decays of ethidium bound to core particles and core particle DNA. Samples were prepared in H_2O at 20 °C. Core particles in (A) 0 M NaCl, (B) 0.01 M NaCl, (C) 0.6 M NaCl, and (D) 1.1 M NaCl. (E) Core particle DNA in 0.1 M NaCl. Samples also contained 0.6 μM core particles or core particle length DNA, 0.18 μM ethidium bromide, and 0.003 mM Tris-HCl (the latter added with the core particles). Data were collected as described in Figure 1.

values of ϕ_{max}. This was not done because experiments run in D_2O similar to those shown in Figure 5A consistently gave a much smaller tyrosine anisotropy change, making interpretation of any results obtained in D_2O questionable. However, the consistency of the values for ϕ_{max} shown by Figure 4 indicates that mean rotational correlation times as high as 400 ns (core particles in 14.2% sucrose at 7 °C) can be estimated with good accuracy from decays with H_2O as the solvent.

The effect of ionic strength on ϕ_{max} values obtained at 0.3 ethidium per core particle is shown in Figure 5B as filled circles. Little variation is observed from 500 mM salt down to 1 mM, a range over which correspondingly little change is seen in the tyrosine anisotropy. Between 1 and 0.1 mM, the tyrosine anisotropy decreases by about half the total change observed while ϕ_{max} increases slowly but correspondingly from ~170 to ~205 ns. Slightly below 0.1 mM, a sharp increase in ϕ_{max} is seen after which the values plateau at ~330 ns below 0.01 mM.

To illustrate the magnitude of the changes observed in the anisotropy decays with changing salt concentration, Figure 6 compares anisotropy decays for ethidium bound to core particles at different ionic strengths. Curves calculated from the recovered decay parameters are shown in order to avoid obscuring the comparison by noise. Curve B is replotted from Figure 3A for core particles in H_2O at 10 mM ionic strength (ϕ_{max} = 159 ns). Curve A was obtained with core particles taken to very low ionic strength (0.003 mM Tris-HCl, ϕ_{max} = 318 ns). In each case, the decay for times greater than ~60 ns is essentially linear, corresponding to depolarization due to rotational diffusion. The curvature below 60 ns, which we attribute to DNA torsional motions, is visibly different for the two samples, being somewhat greater on average for the sample at very low ionic strength.

Core Particle Does Not Open until Irreversible Changes Occur. As long as core particles are not subjected to ionic strengths below 0.2 mM, the low-salt transition as measured by steady-state tyrosine fluorescence appears to be reversible. As the ionic strength is reduced further, progressively greater

Table III: Irreversibility of the Low-Salt Transition

$[M^+]_{min}$[a]	$[M^+]_{final}$[a]	ϕ_{max}	scatter[b]
	0.003	318	
	1	164	0.845
	10	170	0.988
	100	190	1.017
0.003	1	291	0.857
0.003	10	191	0.995
0.003	100	360	1.387
0.4	1	194	
0.3	10	193	
0.3	100	222	

[a] Units are millimolar. Samples were prepared by diluting a concentrated core particle stock (1 mM Tris-HCl, pH 8.2, and 125 μM core particles) into water or NaCl solutions. Absence of a value for $[M^+]_{min}$ indicates that the stock was diluted directly to $[M^+]_{final}$. Otherwise, the dilution was to the indicated minimum cation concentration, $[M^+]_{min}$, followed about 1 h later by the addition of 0.1 volume of an NaCl solution to give $[M^+]_{final}$. The final core particle concentration was about 0.35 μM for all samples. $[M^+]_{min}$ = 0.003 mM represents dilution of the concentrated core particle stock directly into water. This value is calculated from the concentration of Tris-H^+ ions expected to be contributed from the stock solution (without consideration of possible Donnan effect during preparation of the stock which can be expected to result in higher Tris-H^+ concentrations, including those bound to and associated as counterions with the core particles). [b] Relative scatter measured at 90° from the incident beam. The wavelength used was 365 nm.

degrees of irreversible change in the particles can be demonstrated (Libertini & Small, 1987a). The recovered ϕ_{max} (Figure 5B) increases only slightly down to about 0.2 mM; below 0.2 mM, ϕ_{max} increases steeply and plateaus at nearly twice the value measured at moderate ionic strength.

Figure 5A (open circles) shows tyrosine anisotropy results obtained when core particles were first diluted to very low salt concentration and then shifted to higher ionic strengths in the presence of ethidium. The results are very similar to those obtained without ethidium (Libertini & Small, 1987a). Table III lists ϕ_{max} values for such samples; results obtained by dilution directly to the final salt concentrations are included for comparison. For a sample brought from very low salt concentration to 1 mM, ϕ_{max} decreased only slightly, remaining much higher than for a sample diluted directly to 1 mM; thus, core particles with ethidium bound also experience irreversible

effects of exposure to very low salt concentration. The sample taken from low salt concentration to 10 mM gave a much lower ϕ_{max}, indicating refolding; however, the result is significantly higher than the 170 ns obtained by direct dilution to 10 mM salt. These two results are consistent with earlier observations.

Completely unexpected was the result for samples taken from low salt to 100 mM NaCl, which exhibited high values for ϕ_{max}, even larger than the maximum in Figure 5B. Further characterization by electrophoresis of samples on 5% polyacrylamide gels (after concentrating with Amicon microconcentrators), visualized by the usual ethidium staining technique, showed a weak smearing of intensity above the core particle band. The smearing extended to the top of the gel with evidence of one or two discrete bands at about the positions of dimer and trimer nucleosomes. This smearing indicates aggregation of a portion of the core particles. A control sample, diluted directly to 100 mM salt, gave no evidence of aggregation. An equivalent sample taken from very low salt concentration to 10 mM showed evidence of aggregates, but at a much lower level.

The possibility of aggregation was also examined by measurement of scattered light, and the results are included in Table III. A difference is observed only for a final concentration of 100 mM salt. The low level of aggregate indicated by electrophoresis for the sample taken from very low salt to 10 mM may be responsible for the slightly high value of ϕ_{max} obtained. However, it is very unlikely that aggregation can account for the differences in ϕ_{max} obtained at 1 mM ionic strength.

Table III also lists ϕ_{max} for samples taken to salt concentrations within the range of the reversible low-salt transition and then shifted to higher salt. In this case, the results at 1 and 10 mM final salt are indistinguishable and only slightly higher than the controls. Other results suggest that the slight increase in ϕ_{max} derives at least partially from the extra processing required for these samples. For the sample diluted to 0.3 mM and then raised to 100 mM salt, the value of ϕ_{max} is again high; we suspect that this result (and the formation of aggregates evidenced above) arises from transient exposure of the core particles to high salt concentrations during the addition of 0.1 volume of 1.0 M salt needed to attain the final concentration of 0.1 M.

Effects of High Salt Concentration on the Anisotropy Decay. The dependence of ϕ_{max} on salt up to 1.1 M is included in Figure 5B. The recovered ϕ_{max} values show only a small increase in the range of 1–500 mM NaCl followed by a sharp increase at higher salt concentrations. Figure 6 includes curve fits for the anisotropy decays obtained at 0.7 M (curve C) and at 1.1 M salt (curve D). At 500 mM salt, the result would be difficult to distinguish from that at 10 mM (curve B). The progressive shift downward indicates that greater contributions from depolarization due to DNA motions are occurring. For comparison, the anisotropy decay shape obtained for free core particle DNA is included (curve E), and it is apparent that even at 1.1 M salt the result is closer to that for core particles than to the free DNA decay. The source of increased curvature at short times for 0.7 and 1.1 M salt is uncertain since it is possible that the samples contain some free DNA.

Discussion

Is ϕ_{max} a Measure of the Core Particle Rotational Correlation Time? Figure 4 demonstrates that values of ϕ_{max} obtained for ethidium bound to core particles are directly proportional to viscosity and inversely proportional to the temperature, as expected for rotational correlation times at the molecular level. However, the rate and extent of the complex torsional motions of DNA will also increase in magnitude with temperature and be reduced by increases in viscosity, and it would not be surprising if the slower motions of a section of DNA on the core particle responded to temperature and viscosity in a manner similar to rotational motions of the whole core particle. Thus, while demonstration of such linear dependence suggests that ϕ_{max} is a measure of rotational motion of the core particle, this fact alone does not prove it.

Perhaps the best evidence that ϕ_{max} reports accurately on the rotational correlation time is that it is well resolved from the shorter decay lifetimes. This can be seen visually in Figure 3A in that the decays are quite linear over a wide range of time. Torsional flexing appears to make a relatively small contribution to the decay, occurring only at short times. This conclusion is verified by the second paper of this series (Winzeler & Small, 1991) in which a more complex model is used to describe the decay. Even though the data presented in that paper have a much lower signal-to-noise ratio at long times, when fit with the torsional model of Schurr and Schurr the same rotational correlation time is recovered.

Further evidence that we are indeed measuring rotational motion is the fact that the experimental ϕ_{max} values can be predicted with surprising accuracy based on what is known about the shape and size of the core particle. The nucleosome core particle is reported to be approximately cylindrical in shape, with a diameter of 110 Å and a height of 57 Å (Finch et al., 1977; Richmond et al., 1984); this shape can be approximated as an oblate ellipsoid of equivalent volume (5.4×10^5 Å^3) and an axial ratio of about 2 (axes of 64, 127, and 127 Å). Hydrodynamic theory can be used to calculate rotational correlation times (equal to the resultant anisotropy decay lifetimes) for rotational diffusion of ellipsoid-shaped particles in solution. For a general ellipsoid with three unequal axes, five rotational correlation times would normally be expected; however, two pairs of these are virtually equal, and for all practice purposes, there will never be more than three (Small & Isenberg, 1977). For a simple oblate ellipsoid like the core particle, theory shows that there are three correlation times, but these three will be so close that their resolution will not be possible and only an intermediate value will be observed. One would therefore predict a monoexponential anisotropy decay arising from rotational diffusion of the core particle. The rotational correlation time predicted for an oblate ellipsoid of the dimensions given above in water at 20 °C would be ~161 ns, in excellent agreement with the longest anisotropy decay lifetime listed in Table II.

Comparison to Other Results in the Literature. Table IV lists results for the rotational correlation time of core particles at intermediate ionic strengths obtained by different methods. (Our results indicate that ionic strengths between 1 and 500 mM have little effect on the rotational correlation time.) All of the literature values are larger than ours; only the one obtained by Crothers et al. (1978) is in agreement within the estimated uncertainty of the measurement. The studies by Harrington were performed on an early preparation of nucleosomes with a nonhomogeneous DNA length (the length varied from 140 to 180 bp) which may have contributed to the high value obtained. The nucleosome core particles produced by our procedure are highly homogeneous, with a uniform DNA length of about 146 bp. The results of Wang et al. (and those of Schurr and Schurr, who analyzed the same set of data) may have been affected by the high binding ratios used. Wang et al. used an average binding ratio of 2 methylene blue dye molecules per core particle where we generally used

Table IV: Comparison of Our Rotational Diffusion Results with Values from the Literature

source	ϕ_{20}[a]	$D_{sph,20}$[b]	R_s[c]	V_e[d]	h[e]
Crothers et al.[f]	190 ● 50	9×10^5	57	6.4×10^5	1.2
Harrington[g]	353	4.72×10^5	70	15.0×10^5	3.8
Wang et al.[h]	300	5.6×10^5	66	10.0×10^5	2.3
Schurr and Schurr[i]	272.4	6.118×10^5	64	9.2×10^5	2.1
our work[j]	164 ± 3	10.2×10^5	54	5.6×10^5	1.0

[a] ϕ_{20} is the observed mean rotational correlation time in nanoseconds (corrected to 20 °C). [b] $D_{sph,20}$ is the rotational diffusion coefficient (s^{-1}; $6D_{sph,20} = 1/\phi_{20}$). This equation assumes that the core particle is an isotropic rotator (i.e., it has only one rotational correlation time). This is true for a sphere and is a good approximation for oblate ellipsoids of rotation (Small & Isenberg, 1977). [c] R_s is the radius in angstroms of a sphere which would have the reported rotational diffusion properties (assuming a viscosity of 1.0 cP). $\phi_{20} = \eta V_s/kT$, with $V_s = (4/3)\pi R_s^3$; k = Boltzmann's constant, T = the absolute temperature. [d] V_e is the volume (in Å^3) of an oblate ellipsoid of rotation with an axial ratio of 2.0, which would have the given mean rotational correlation time at 20 °C. V_e can be calculated by using the well-known properties of ellipsoids of rotation (Koenig, 1975), although we use more general expressions (Small et al., 1988). V_e can be compared with 5.4×10^5 Å^3, the volume of the 110 × 57 Å disk proposed as the shape of the core particle [reviewed by van Holde (1988)] by crystallographic studies. [e] h is the degree of hydration (grams of water per gram of core particle) necessary to have a final hydrated volume of V_e. The hydrated volume is assumed to be $V_e = M(\bar{v} + h)/N$, where M is the molecular weight (204 000), N is Avogadro's number, and $\bar{v}$ is the partial specific volume [0.662 cm^3/g; from Greulich et al. (1985)]. [f] Using electric dichroism, Crothers et al. (1978) report a rotational relaxation time of 0.8 ● 0.2 μs measured on core particles obtained by nuclease digestion of H1-depleted calf thymus chromatin. Measurements were performed in 2.5 mM Tris-HCl/1.25 mM Na_2EDTA at pH 7.6 and 7 °C. Correcting for the viscosity difference between 7 and 20 °C and dividing by 3 to convert the relaxation time to a correlation time, we obtain the approximate value of ϕ_{20} shown. [g] Using flow birefringence, Harrington (1981) reports a rotational diffusion coefficient of 4.19×10^5 s^{-1} for nucleosomes at 25 °C in 100 mM KCl and 0.2 mM EDTA at an unspecified pH. Correcting for the viscosity difference between 25 and 20 °C and converting to a correlation time ($\phi = 1/6D$), we obtain the ϕ_{20} value shown. [h] Using triplet-state anisotropy decay of methylene blue intercalated into the DNA of core particles, Wang et al. (1982) report a rotational correlation time for core particles of 450 ns at 5 °C with ~2 dye molecules bound per core particle. The particles were isolated after micrococcal nuclease treatment of chicken erythrocyte nuclei, and solution conditions are reported to be 10 mM Tris-HCl and 0.05 mM Na_2EDTA at pH 7.8. The reported value of ϕ_{20} was corrected for the viscosity difference between 5 and 20 °C. [i] Schurr and Schurr (1985) fit the same data set presented originally by Wang et al. (1982) and report a rotational diffusion coefficient of 4.036×10^5 s^{-1}, yielding nearly the same correlation time reported by the original workers. [j] These are our values determined by using the fluorescence anisotropy decay of intercalated ethidium. The value presented for ϕ_{20} is the mean of five separate determinations made on different days; conditions were as described in Figure 1, except that the ethidium concentration was 0.18 μM. The reported error is plus or minus one standard deviation calculated from the five determinations.

a ratio of 0.3. No data are available on the effect of methylene blue binding on core particle structure. Ethidium binding ratios up to about 1.5 per core particle are reported to have little effect on the structure as judged by electric dichroism and sedimentation measurements (Wu et al., 1980). Higher ratios induce a transition to a more open structure (Wu et al., 1980) and can cause partial or total dissociation of histones from the core particle (McMurray & van Holde, 1986). We have found that ϕ_{max} is relatively independent of the ethidium binding ratio up to about 2 ethidium molecules per core particle (data not shown). However, effects on the shorter decay lifetimes become apparent above 0.3 ethidium per core particle (Winzeler & Small, 1991).

Reversible Low-Salt Transition. When the ionic strength is reduced below 3 mM, a number of physical properties of core particles begin to show changes which suggest a significant expansion of the particle at very low salt concentration. The ionic strength range involved and the magnitude of the changes vary somewhat depending on the methods used to characterize the transition, on the homogeneity in the length of the DNA, and on the pH [see van Holde (1988) for a discussion of possible reasons for the differences]. For core particles prepared by our methods, we have consistently observed a transition centered below 0.5 mM salt when a concentrated core particle stock solution, transferred to low salt (e.g., 1 mM Tris-HCl, pH 7.5), was diluted into water containing various salt concentrations (Libertini & Small, 1980, 1982, 1984a, 1987a; Libertini et al., 1988). The pH for such samples typically varies between 6 and 7. The transition showed similar properties whether characterized by fluorescence intensity and anisotropy of intrinsic tyrosine residues, by sedimentation in the ultracentrifuge, or by circular dichroism of the DNA at 283 nm.

Figure 5A illustrates the dependence of core particle tyrosine fluorescence anisotropy on ionic strength. The results obtained when the core particle stock was diluted directly to the indicated [M^+] were independent of the presence (filled circles) or absence (plus symbols) of the 0.3 ethidium molecule per core particle used in the majority of our anisotropy decay measurements. The transition appears to be centered near 0.2 mM. Figure 5B shows the dependence of ϕ_{max} for samples prepared in the same manner. The values of ϕ_{max} are essentially independent of [M^+] over the right half of the tyrosine anisotropy changes. It is interesting that this range ([M^+] >0.2 mM) corresponds to that over which the tyrosine anisotropy changes have appeared to be reversible (Libertini & Small, 1987a). The small increase in ϕ_{max} as [M^+] is decreased from 10 mM down to ~0.2 mM suggests that the structural changes which are the source of the reversible tyrosine anisotropy changes have a relatively minor effect on the shape of the core particle.

Irreversible Changes at Very Low Salt Concentration. If the concentrated core particle stock is first diluted to very low salt ([M^+] <0.2 mM) before samples are prepared, the shape of the resulting curve of tyrosine anisotropy vs ionic strength is different (Libertini & Small, 1987a; Libertini et al., 1988), indicating that the effects of such low salt are not reversible. This irreversibility is illustrated by the open circles in Figure 5A. Again, the presence of ethidium at 0.3 per core particle had little effect on the shape of the curve obtained.

Earlier work demonstrated that the irreversibility requires reduction of [M^+] to below 0.2 mM and becomes progressively more marked as the ionic strength decreases further (Libertini & Small, 1987a). The major changes in ϕ_{max} at low ionic strength are seen to occur between about 0.05 and 0.2 mM. This correlation suggests that whatever happens to the core particle to induce the irreversibility is accompanied by a significant change in the shape or volume of the particle.

Near 1 mM salt, the tyrosine anisotropy values in Figure 5A (open circles) suggest that many of the core particles cycled through very low salt remain in the state induced by that exposure. This conclusion is supported by ethidium anisotropy decay measurements; the ϕ_{max} value (291 ns, Table III) remains much higher than that obtained when the core particle stock was diluted directly to 1 mM (164 ns). When exposed to very low salt and then taken to 10 mM, the final tyrosine anisotropy indicates that the particles are now much more similar to particles taken directly to 10 mM (Figure 5A). In agreement, the ϕ_{max} value after initial exposure to very low salt (191 ns) is much closer to the control (170 ns). Evidence from electrophoresis and light scattering indicates that the surprisingly high value of ϕ_{max} obtained at 100 mM salt after

exposure to very low salt is an artifact due to formation of significant amounts of aggregates during the addition of 1 M salt.

Shape of the Core Particle at Very Low Ionic Strength. As mentioned earlier in this section, the core particle at moderate ionic strength (10 mM, $\phi_{max} \sim 164$ ns) can be modeled by an oblate ellipsoid of axial dimensions 64,127,127 Å, a shape consistent with what is known about the structure. The increase in ϕ_{max} to 330 ns at very low ionic strength clearly indicates that low salt induces a dramatic change in the shape of the core particle. In order to examine the shapes attainable by the core particle and consistent with a 330-ns mean rotational correlation time, we model them using a hydrodynamically equivalent ellipsoid, the ellipsoid which has the same principle rotational diffusion coefficients as the core particle. We expect the shape of such an ellipsoid to correspond roughly to the actual shape of the core particle.

The oblate ellipsoid of rotation model that we use for the native core particle has three rotational correlation times, all nearly equal. In order for the core particle at very low ionic strength to retain a shape which can be modeled by an oblate ellipsoid (without a change in total volume) and have a rotational correlation time of 330 ns, the equivalent ellipsoid would have to be flattened from an axial ratio of 2 to a ratio closer to 5 (axial dimensions 35,173,173 Å). If we assume that the DNA remains on the outside of such a model, then the core particle would have to open until the DNA follows a roughly circular path without overlap at the ends. This model is very similar to one shown by Wu et al. (1979) to be consistent with transient electric dichroism measurements on core particles at low salt. Oblate ellipsoid models having axial ratios less than 5 are possible, but would require a substantial increase in the total volume. For example, in the relatively extreme case of maintaining an axial ratio of 2, the total volume would have to be increased by 100%. Smaller increases would be needed with larger axial ratios. However, the only reasonable mechanism for a volume increase would be further hydration of the core particle, which seems unlikely given the already high degree of hydration that we attribute to the particle in the native form based on the volume of a cylinder 57 Å high and 110 Å in diameter (1.0 g of H_2O/g of core particle).

For prolate ellipsoids of rotation or elongated general ellipsoids, the three correlation times for a given volume and axial ratio can be widely separated (there are actually five correlation times for the general ellipsoid, but two pairs of these are degenerate). If more than one rotational correlation time can be demonstrated in an anisotropy decay, then the use of an elongated ellipsoid model is indicated. However, where resolution of only a single correlation time is possible, use of a prolate model presents special problems since the average decay lifetime expected will be strongly dependent on the orientation of the emission dipole of the probe with respect to the long axis of the ellipsoid. In this case, without assumptions other than that the volume remains constant, one can only put a lower limit on the axial ratio required to give the experimental correlation time (corresponding to the probe emission moment parallel to the long axis). For a prolate ellipsoid having a volume equal to that of the core particle, this lower limit is about 3 (axial dimensions of about 210,70,70 Å) since smaller axial ratios cannot give a rotational correlation time as large as 330 ns. An upper limit on the axial ratio cannot be established since two of the five correlation times of a prolate ellipsoid are comparable to that of a sphere of the same volume, even for physically unreasonable ratios. In the case of ethidium bound to the DNA of a core particle, one could consider the likelihood that many different binding sites for the probe exist with various orientations. In such a case, the observed rotational correlation time might approximate an average of the five predicted values. Given this assumption, the axial ratio giving an average of 330 ns would be about 5 (axial dimensions 296,59,59 Å).

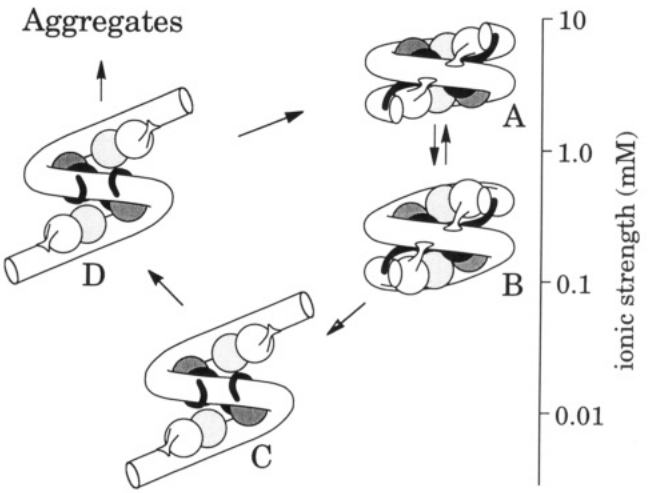

FIGURE 7: Cartoon interpretation of the structure of the nucleosome core particle at various steps in the low-salt transition. Core histones are represented as follows: black = H3; gray = H4; light gray = H2B; white = H2A. The locations indicated for the "crossbinding" interactions (see text) shown for H2A and H3 with the DNA in structure A are based on the results of Shick et al. (1980). However, the manner in which they are drawn is intended to represent nothing more than the adoration shared by all histones for DNA.

Figure 7 is a diagrammatic representation of the changes which may be occurring during the low-salt transition. Structure A is the native form of the core particle typically found at intermediate salt (~10 mM). This structure includes reported H2A (white) contacts with the DNA near the center of the 145 bp DNA and H3 (black) interactions near the 3′ ends. Each histone also interacts with the DNA in the general area of its location on the inside of the superhelix, but only H2A and H3 show such "crossbinding" interactions in a separate region far from the local sites (Shick et al., 1980).

The driving force for the low-salt transition is thought to be electrostatic repulsion between adjacent turns of the DNA. The physical forces resisting this repulsion are the interactions among the histones and the interactions between the histones and DNA such as those specifically diagrammed. In the absence of DNA, the core histones interact strongly to form a tetramer, $(H3–H4)_2$, and a dimer, H2A–H2B; interactions between the tetramer and dimer are weaker and require very high ionic strengths, presumably because of the high overall positive charge on these proteins. Ionic histone–DNA interactions will become stronger with decreasing salt concentration and will tend to resist the opening of the particle. Structure B in Figure 7 represents a form of the core particle which might be involved in the reversible phase of the low-salt transition. This representation is based on the assumption that it is the weak interactions between H2A–H2B and $(H3–H4)_2$ which break first and decrease the electrostatic repulsion somewhat by allowing adjacent turns of the DNA to move further apart, and is in agreement with the results of Martinson et al. (1979) where contact-site cross-linking experiments showed that specific interactions between H2B and H4 are broken when nucleosomes are exposed to very dilute buffers. Reversibility of this phase of the transition can be anticipated since the overall shape of the molecule changes little and

interactions between the histone dimers and tetramers can be easily reestablished when the ionic strength is increased. This model is consistent with the relatively small changes in ϕ_{max} observed over the reversible portion of the low-salt transition ([M^+] >0.1 mM in Figure 5). Partial separation of the dimers from the tetramer can account for the lower tyrosine fluorescence anisotropy of the complex at low salt concentration since histones in the absence of DNA give a high anisotropy at high salt (2 M NaCl), where the dimers and tetramers interact, and a lower anisotropy at low salt (0.5 M), where they do not (unpublished results).

The doubling of ϕ_{max} as the ionic strength is decreased further indicates a more dramatic opening of the core particle. In structure B, we propose that the "crossbinding" interactions of H2A and H3 with the DNA play a role in holding the particle in its near-native shape, and we suggest that it is these interactions which are broken at very low salt concentration. Structure C illustrates one end of a continuum of possible shapes which might evolve when the "crossbinding" interactions are disrupted. The other end of the continuum would consist of a straight DNA strand with the histones spread along it. The structure illustrated was chosen because it would require little change in the histone–histone interactions within the dimers and tetramers, or in the interactions between them and the DNA, since much of the curvature of the DNA is preserved. In addition, the extended structure shown is consistent with recent electron spectroscopic imaging results obtained for hyperacetylated HeLa cell core particles at low salt (Oliva et al., 1990).

Irreversible Low-Salt Transition. More significant than the shape in Figure 7C is the fact that, once ionic interactions within the core particle are broken at the extremely low ionic strengths required, the sections of the histones involved will likely find different regions of the DNA to bind to, as illustrated. The possibility that interparticle interactions might occur at very low salt seems remote since the high overall negative charge on the core particles would keep them apart. Such "secondary" ionic binding could be quite strong and unlikely to rearrange at a significant rate until the ionic strength is increased to values well above those needed to induce the first evidence of the low-salt transition. Our measurements suggest that these "secondary" ionic bonds do not become labile until the salt concentration is jumped to between 1 and 10 mM. At 1 mM, the ϕ_{max} value obtained for samples cycled through very low salt (~290 ns) was not much less than the result at very low salt (~330 ns); this observation is represented in Figure 7 by structure D, which is like structure C. The decrease may be due to a mixture of refolded and open particles or to partial compaction of the average particle as compared with structure C (recall that structure C, and likewise structure D, represents only one of many shapes which would be consistent with the observed correlation times). With a final salt concentration of 10 mM, the ϕ_{max} was reduced considerably, and electrophoresis indicated that most of the resulting complexes migrate like native core particles. The remaining material appeared to aggregate to give a slower migrating, diffuse background, presumably due to interparticle ionic bond formation and to entanglement. The amount of background produced was much greater when the salt concentration was jumped to 100 mM. This might be due to partial dissociation of core particles as the low-salt sample was mixed with 1 M salt (suggested by evidence of free DNA) or due to differences in the relative rates of dissociation of the "secondary" ionic bonds and refolding of the core particles.

Core Particles at High Salt Concentration. The nucleosome core particle is a complex of proteins bound to DNA largely through ionic interactions. With increasing ionic strength, the protein–DNA interactions become weaker, and as the salt concentration is increased above 0.8 M, a stepwise dissociation of the histones can be observed, beginning with release of the H2A–H2B dimers (Burton et al., 1978; Jorcano & Ruiz-Carillo, 1979). The large value of ϕ_{max} obtained at 1.1 M salt (Figure 5B) may arise at least partially from species lacking one or both dimers. Ethidium would be expected to bind to the relatively unrestricted DNA vacated by the dimers and give rise to the more rapid depolarization at short times shown in Figure 6 (curve D).

Below 0.75 M salt, a *very slow*, cooperative dissociation to free DNA and histones can be observed, the extent increasing with ionic strength to ~17% at 0.5 M salt (Yager et al., 1989). The extent of dissociation also depends on the core particle concentration; the value of 17% free DNA is valid at 0.15 μM core particles but becomes almost insignificant above 0.5 μM (our experiments were done at 0.35 μM or higher). Thus, the anisotropy decays for core particles at high salt may contain contributions from ethidium bound to free DNA.

In addition to this slow, limited dissociation, core particles have been shown to undergo a much faster transition in the salt range 0.3–0.7 M characterized by changes in sedimentation coefficient and circular dichroism of the DNA (Ausió & van Holde, 1986; Yager et al., 1989). These authors proposed that this predissociation transition involves freeing of the ends of the DNA with increasing salt without significant dissociation of histones. We have been unable to clearly demonstrate this transition with histone tyrosine fluorescence measurements. Although small changes in the tyrosine intensity and anisotropy are evident over this salt range, they are continuous with the effects of rapid dissociation above 0.8 M salt and do not clearly demonstrate a predissociation transition [see, for example, Figure 4 of Libertini et al. (1988)].

The ethidium anisotropy decay results in Figure 5B indicate no change in ϕ_{max} up to 0.5 M salt. Above 0.5 M, ϕ_{max} rises steeply (~240 ns at 0.6 and 0.9 M salt and >300 ns at 1.1 M). The anisotropy decay at 1.1 M salt (curve D in Figure 6) indicates a large increase in contributions from shorter decay times, probably due to increased flexibility of the DNA. The high ϕ_{max} is consistent with a partially dissociated DNA–histone complex which is expanded in relation to the compact core particle. In contrast, the decay observed at 0.6 M salt (curve C, Figure 6) suggests little change in DNA flexibility, consistent with an intact particle. The increase in ϕ_{max} then would indicate a significant expansion of the particle which might correspond to the predissociation transition. More extensive characterization of this salt range, including effects of pH which differ between our experiments and those of other workers, is in progress and will be published separately.

Conclusions

In this paper, we have examined the fluorescence anisotropy decay of ethidium bound to nucleosome core particles. This fluorescent probe has a lifetime sufficiently long to allow the measurement of the rotational correlation time of a large molecular complex such as a nucleosome core particle. In addition, this lifetime can be nearly doubled through the use of D_2O as the solvent, allowing the measurement of anisotropy decays at much longer times than with H_2O, and thus providing greater confidence in the measurement of rotational diffusion. Through analysis of these anisotropy decays, we are able to measure the rotational correlation time of the core particle in solution and show that our results agree quite well

with the dimensions as determined by other means. In addition, we can make qualitative statements about the shape of the core particle under various conditions, such as varying ionic strength. Experiments done at varying ionic strengths show that the nucleosome core particle opens to an extended structure at ionic strengths below 0.2 mM where nonreversible effects are observed.

References

Ashikawa, I., Kinoshita, K., Jr., Ikegami, A., Nishimura, Y., Tsuboi, M., Watanabe, K., Iso, K., & Nakano, T. (1983) *Biochemistry 22*, 6018–6026.

Ausió, J., & van Holde, K. E. (1986) *Biochemistry 25*, 1421–1428.

Bevington, P. R. (1956) *Data Reduction and Error Analysis for the Physical Sciences*, McGraw-Hill, New York.

Brown, D. W., Libertini, L. J., & Small, E. W. (1990) *Proc. SPIE—Int. Soc. Opt. Eng. 1204*, 380–391.

Burch, J. B. E., & Martinson, H. G. (1980) *Nucleic Acids Res. 8*, 4969–4987.

Burton, D. R., Butler, M. J., Hyde, J. E., Phillips, D., Skidmore, C. J., & Walker, I. O. (1978) *Nucleic Acids Res. 5*, 3643–3663.

Covington, A. K., Paabo, M., Robinson, R. A., & Bates, R. G. (1968) *Anal. Chem. 40*, 700–706.

Crothers, D. M., Dattagupta, N., Hogan, M., Klevan, L., & Lee, K. S. (1978) *Biochemistry 17*, 4525–4533.

Finch, J. T., Lutter, L. C., Rhodes, D., Brown, R. S., Rushton, B., Levitt, M., & Klug, A. (1977) *Nature (London) 269*, 29–36.

Genest, D., Wahl, P., Erard, M., Champagne, M., & Daune, M. (1982) *Biochimie 64*, 419–427.

Greulich, K. O., Ausió, J., & Eisenberg, H. (1985) *J. Mol. Biol. 186*, 167–173.

Harrington, R. E. (1981) *Biopolymers 20*, 719–752.

Hirai, M., Niimura, N., Zama, M., Mita, K., Ichimura, S., Tokunaga, F., & Ishikawa, Y. (1988) *Biochemistry 27*, 7924–7931.

Hirose, M. (1988) *J. Biochem. 103*, 31–35.

Hutchings, J. J., & Small, E. W. (1990) *Proc. SPIE—Int. Soc. Opt. Eng. 1204*, 184–191.

Isenberg, I. I., & Small, E. W. (1982) *J. Chem. Phys. 77*, 2799–2805.

Jorcano, J. L., & Ruiz-Carillo, A. (1979) *Biochemistry 18*, 768–774.

Koenig, S. (1975) *Biopolymers 14*, 2421–2423.

Libertini, L. J., & Small, E. W. (1980) *Nucleic Acids Res. 8*, 3517–3534.

Libertini, L. J., & Small, E. W. (1982) *Biochemistry 21*, 3327–3334.

Libertini, L. J., & Small, E. W. (1983) *Rev. Sci. Instrum. 54*, 1458–1466.

Libertini, L. J., & Small, E. W. (1984a) *Nucleic Acids Res. 12*, 4351–4359.

Libertini, L. J., & Small, E. W. (1984b) *Anal. Biochem. 138*, 314–318.

Libertini, L. J., & Small, E. W. (1987a) *Nucleic Acids Res. 15*, 6655–6664.

Libertini, L. J., & Small, E. W. (1987b) *Anal. Biochem. 163*, 500–505.

Libertini, L. J., & Small, E. W. (1989) *Biophys. Chem. 34*, 269–282.

Libertini, L. J., Ausió, J., van Holde, K. E., & Small, E. W. (1988) *Biophys. J. 53*, 477–487.

Magde, D., Zappala, M., Knox, W. H., & Nordlund, T. M. (1983) *J. Phys. Chem. 87*, 3286–3288.

Martinson, H. G., True, R. J., & Burch, J. B. E. (1979) *Biochemistry 18*, 1082–1089.

Matsunaga, N., & Nagashima, A. (1983) *J. Phys. Chem. Ref. Data 12*, 933–966.

McMurray, C. T., & van Holde, K. E. (1986) *Proc. Natl. Acad. Sci. U.S.A. 83*, 8472–8476.

Millar, D. P., Robbins, R. J., & Zewail, A. H. (1980) *Proc. Natl. Acad. Sci. U.S.A. 77*, 5593–5597.

Mita, K., Zama, M., Ichimura, S., Niimura, N., Kaji, K., Hirai, M., & Ishikawa, Y. (1983) *Physica 120B*, 436–439.

Oliva, R., Bazett-Jones, D. P., Locklear, L., & Dixon, G. H. (1990) *Nucleic Acids Res. 18*, 2739–2747.

Olmsted, J., III & Kearns, D. R. (1977) *Biochemistry 16*, 3647–3654.

Richmond, T. J., Finch, J. T., Rushton, B., Rhodes, D., & Klug, A. (1984) *Nature (London) 311*, 532–537.

Schurr, J. M. (1984) *Chem. Phys. 84*, 71–96.

Schurr, J. M., & Schurr, R. L. (1985) *Biopolymers 24*, 1931–1940.

Shick, V. V., Belyavsky, A. V., Bavykin, S. G., & Mirzabekov, A. D. (1980) *J. Mol. Biol. 139*, 491–517.

Small, E. W. (1991a) in *Modern Fluorescence Spectroscopy: Principles and Techniques* (Lakowicz, J. R., Ed.) Vol. 1, Plenum Press, New York (in press).

Small, E. W. (1991b) in *Numerical Computer Methods* (Brand, L., & Johnson, M. L., Eds.) Academic Press, Orlando, FL (in press).

Small, E. W., & Isenberg, I. I. (1977) *Biopolymers 16*, 1907–1928.

Small, E. W., & Anderson, S. R. (1988) *Biochemistry 27*, 419–428.

Small, E. W., Libertini, L. J., & Small, J. R. (1988) *Proc. SPIE—Int. Soc. Opt. Eng. 909*, 97–107.

Small, E. W., Libertini, L. J., Brown, D. W., & Small, J. R. (1989) *Proc. SPIE—Int. Soc. Opt. Eng. 1054*, 36–53.

Small, E. W., Libertini, L. J., Brown, D. W., & Small, J. R. (1991) *Opt. Eng. 30*, 345–356.

Uberbacher, E. C., Ramakrishnan, V., Olins, D. E., & Bunick, G. J. (1983) *Biochemistry 22*, 4916–4923.

van Holde, K. E. (1988) *Chromatin*, Springer-Verlag, New York.

Wahl, P., Paoletti, J., & LePecq, J.-B. (1970) *Proc. Natl. Acad. Sci. U.S.A. 65*, 417–421.

Wang, J., Hogan, M., & Austin, R. H. (1982) *Proc. Natl. Acad. Sci. U.S.A. 79*, 5896–5900.

Winzeler, E. A., & Small, E. W. (1991) *Biochemistry* (following paper in this issue).

Wu, H.-M., Dattagupta, N., Hogan, M., & Crothers, D. M. (1979) *Biochemistry 18*, 3960–3965.

Wu, H.-M., Dattagupta, N., Hogan, M., & Crothers, D. M. (1980) *Biochemistry 19*, 626–634.

Yager, T. D., McMurray, C. T., & van Holde, K. E. (1989) *Biochemistry 28*, 2271–2281.